Effect of Solvent Annealing on the Tensile Deformation Mechanism of a Colloidal Crystalline Polymeric Latex Film

ARTICLE *in* LANGMUIR · AUGUST 2011

Impact Factor: 4.46 · DOI: 10.1021/la2026939 · Source: PubMed

7 AUTHORS, INCLUDING:

Jianqi Zhang
National Center for Nanoscience and Techn…
31 PUBLICATIONS **93** CITATIONS
SEE PROFILE

Rainer Gehrke
Deutsches Elektronen-Synchrotron
170 PUBLICATIONS **1,572** CITATIONS
SEE PROFILE

Yongfeng Men
Chinese Academy of Sciences
86 PUBLICATIONS **1,405** CITATIONS
SEE PROFILE

Langmuir

ARTICLE

pubs.acs.org/Langmuir

Effect of Solvent Annealing on the Tensile Deformation Mechanism of a Colloidal Crystalline Polymeric Latex Film

Jianqi Zhang,[†] Zhiyong Yi,[†] Qiao Wang,[†] Zhenyu Liu,[‡] Jan Perlich,[§] Rainer Gehrke,[§] and Yongfeng Men*[,†]

[†]State Key Laboratory of Polymer Physics and Chemistry, Changchun Institute of Applied Chemistry, Chinese Academy of Sciences, Renmin Street 5625, 130022 Changchun, PR China

[‡]State Key Laboratory of Applied Optics, Changchun Institute of Optics, Fine Mechanics and Physics (CIOMP), Chinese Academy of Sciences, 130033 Changchun, China

[§]HASYLAB am DESY, Notkestrasse 85, 22607 Hamburg, Germany

ABSTRACT: The influence of solvent annealing on microscopic deformational behavior of a styrene/n-butyl acrylate copolymer latex film subjected to uniaxial tensile deformation was studied by small-angle X-ray scattering. It was demonstrated that the microscopic deformation mechanism of the latex films transformed from a nonaffine deformation behavior to an affine deformation behavior after solvent annealing. This was attributed to the interdiffusion of polymeric chains between adjacent swollen latex particles in the film. It turns out that solvent annealing is much more efficient than thermal annealing due to a much slow evaporation process after solvent annealing.

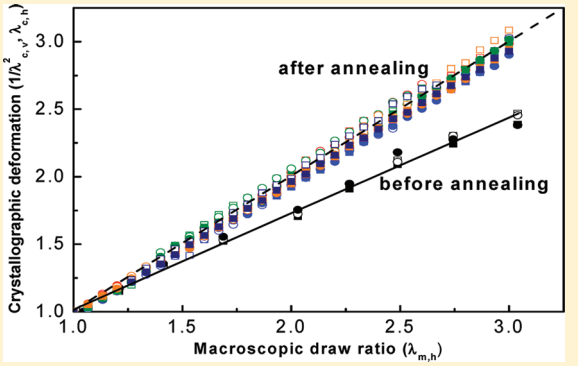

INTRODUCTION

Films obtained via drying a polymeric latex dispersion are normally colloidal crystalline where latex particles are packed into a face-centered cubic (fcc) structure.[1−5] Different from conventional atomic or hard sphere colloidal crystallites, the crystalline structure of these films is normally deformable because of the low glass-transition temperature of the constituent polymers in latex particles. The film-formation process during water evaporation has been considered in terms of three sequential steps including close packing of the latex particles, particle deformation, and polymer interdiffusion between adjacent particles.[6−8] Polymer diffusion across the interparticle boundaries can provide effective adhesive forces between particles that give more strength to the film. The extent of interdiffusion of polymer chains across the interface has been investigated by small-angle neutron scattering (SANS) and fluorescence techniques.[7,9,10] Studies on the effect of temperature,[9] molecular weight,[10] polymer composition,[11,12] the influence of coalescing aids (volatile organic solvents),[13] nonionic surfactants,[14,15] and the influence of latex structure on the interdiffusion process have been performed.[16−18]

Although the film-formation process of latex dispersions has been widely studied, only a few investigations were focused on the deformation mechanism of polymer latex films in view of microstructure evolution. Because the building blocks of latex colloidal crystallites are very large with a typical size on the order of 100 nm, SANS and small-angle X-ray scattering (SAXS) are predominant techniques for studying their microstructural evolution during deformation. The deformation of composite films, derived from drying latex dispersions yielded by mechanical mixing or in situ filler synthesis, was studied by means of SANS, and a theoretical model was presented.[19] Lepizzera et al.[20] presented evidence for two modes of deformation based on atomic force microscopy studies on deformed core/shell latex films: matrix deformation and geometric rearrangement. A study of the rheological properties of silica-filled nanolatex films by means of uniaxial strain experiments was presented by Oberdisse,[21] where it was pointed out that silica contributes differently at small and large deformations. Cabane et al. studied the deformation of cellular polymeric latex films by means of SANS and elucidated that the deformation of the films was affine when the films were stretched in the dry state whereas macroscopic stretching caused microscopic shear deformation (i.e., the particles slipped past each other in the wet state).[22] Often, the use of SANS requires enhanced contrast in the system under investigation by adding D_2O. It has been illustrated that SAXS seems to be the ideal technique for such an investigation. This is primarily due to the already existing contrast between polymeric latex particles and additives such as salt, emulsifiers, and so on located in the interstices after film formation.[23−30] The deformation mechanism of soft latex films with colloidal polycrystalline and fiber symmetric crystalline

Received: July 14, 2011
Revised: August 28, 2011
Published: August 29, 2011

dx.doi.org/10.1021/la2026939 | *Langmuir* 2011, 27, 12197–12200

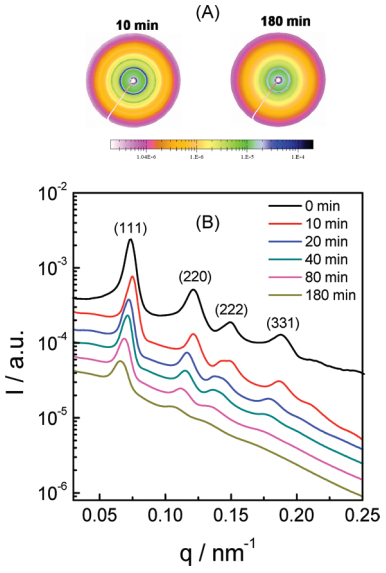

Figure 1. (A) SAXS patterns for samples annealed for 10 and 180 min in solvent. (B) Integrated 1D SAXS intensity distributions of the undeformed latex films.

structure was studied by SAXS.[23,26−28] It was found that the crystalline lattice constants change considerably during macroscopic deformation, resulting not only in the deformation of the crystallographic structure but also in considerable nonaffine deformation at high draw ratios. The deformation behavior of the latex films changes from nonaffine to affine deformation with increasing annealing temperature, which can be attributed to the diffusion of polymeric chains between adjacent latex particles resulting in an enhancement of the cohesive bonding between particles in the crystallites and at the grain boundaries.

Practically, in order to enhance the strength of latex painting, coalescing aids are used because it is difficult to apply thermal annealing over a large area. The aim of this work is therefore to check for the effect of solvent annealing on microstructural evolution during the tensile deformation of a colloidal crystalline polymeric latex film. In situ SAXS measurements taken during stretching runs indicated that the deformation mechanism of the latex films transformed from nonaffine deformation to affine deformation after solvent annealing in a much more pronounced manner than after thermal annealing at elevated temperatures. This behavior indicates that the presence of an organic solvent in the latex film promotes the interdiffusion of polymeric chains between adjacent particles to a larger extent than by using thermal annealing.

EXPERIMENTAL SECTION

A commercially available styrene/*n*-butyl acrylate copolymer (PS-*co*-BA) latex dispersion with a solid content of ca. 40 wt % provided by BASF China was used. The glass-transition temperature of this PS-*co*-BA is 20 °C. The diameter of the latex particles is 118 nm as determined by SAXS. The latex films were obtained by evaporating the water from the latex dispersion under ambient conditions (25 °C and 30% relative humidity) for 2 weeks, yielding a transparent film of about 1 mm thickness. The samples were cut into pieces with 25 mm length and 6 mm width. Then they were immersed in a mixed solvent composed of acetone and water (the volume ratio of acetone to water is 15) for 10, 20, 40, 80, and 180 min, respectively. The samples were then picked out of the solvent and were dried again by placing them in air with one side of the films stuck to a glass plate.

Thermogravimetric analysis (TGA) was carried out using a Mettler Toledo TGA-SDTA851 analyzer (Switzerland) from 25 to 800 °C in a nitrogen flow of 20 mL/min at a heating rate of 10 K/min. The setup was also used to observe the evaporation process after solvent annealing. In that case, the weight of a small piece of sample (13.48 mg before solvent annealing) was measured after 20 min of solvent annealing as a function of time at room temperature.

Synchrotron SAXS measurements were performed at beamline BW4 at HASYLAB, DESY, Hamburg, Germany. The energy of the X-ray radiation was 8.979 keV, resulting in a wavelength of 0.13808 nm. The size of the primary X-ray beam at the sample position was $0.4 \times 0.4\ mm^2$. The sample was mounted onto a tensile tester at the beamline at a sample-to-detector distance of 13 920 mm. At this distance, the effective scattering vector q ($q = 4\pi/(\lambda \sin \theta)$, where 2θ is the scattering angle and λ is the wavelength) range is $0.02-0.25\ nm^{-1}$. The samples were stretched at a speed of 30 μm/s. The samples were stretched at both ends, ensuring that the X-rays were scattered at a fixed position in the middle of the sample. Each SAXS pattern was collected within 60 s during a continuous stretching run. The SAXS data were calibrated for background scattering and normalized with respect to the primary beam intensity.

RESULTS AND DISCUSSION

Figure 1A presents SAXS patterns for samples annealed for 10 and 180 min in solvent. Two characteristic features can be identified. First, the scattering intensity decreased with increasing annealing time, which can be attributed to the gradual loss of contrast in the films resulting from the dissolution of salts and surfactants from the interstices of particles in the latex films by solvent. Evidence for such a process can be shown by TGA results, which will be discussed in detail below. Second, diffraction rings became smaller at longer annealing times. To demonstrate the changes in q values at diffraction positions quantitatively, 1D SAXS intensity distributions of the latex films are plotted in Figure 1B. In the diagram, only relative intensities are given and spectra are vertically shifted for the sake of clarity. The Miller indices of the corresponding peaks are given in the plot by considering an fcc colloidal crystalline structure. The shift of the corresponding peak positions to larger q values at shorter annealing times and to smaller q values at longer annealing times is clearly identifiable. As for the shift in the corresponding q positions to larger values, this behavior is explained by assuming the occurrence of particle coalescence accompanied by dissolving material that is not compatible with the latex polymers, such as surfactants that initially cover the surfaces of the latex particles, in the solvent during solvent annealing. With respect to the shift in the corresponding q positions to smaller values, it may have two origins: either residual solvents still exists in the latex films (films might have not completely redried after 7 days), resulting in latex particles still being in a swollen state, or latex films are deformed during the redrying process (i.e., they were compressed in the thickness direction that is parallel to the incident X-ray beam during SAXS measurements). To verify the actual reasons, TGA measurements were conducted. Figure 2A presents TGA results of a nonannealed film (solid line) and a film annealed in solvent for 180 min (dashed line). The two TGA curves are almost overlapping until decomposition occurs, indicating no detectable solvent left in the latex film after redrying. Therefore,

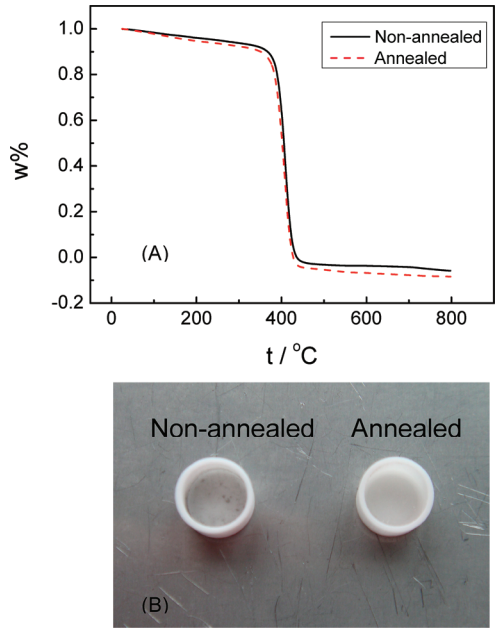

Figure 2. (A) Normalized themogravimeric curves for nonannealed and annealed latex films. (B) Photograph of crucibles used in the TGA experiment.

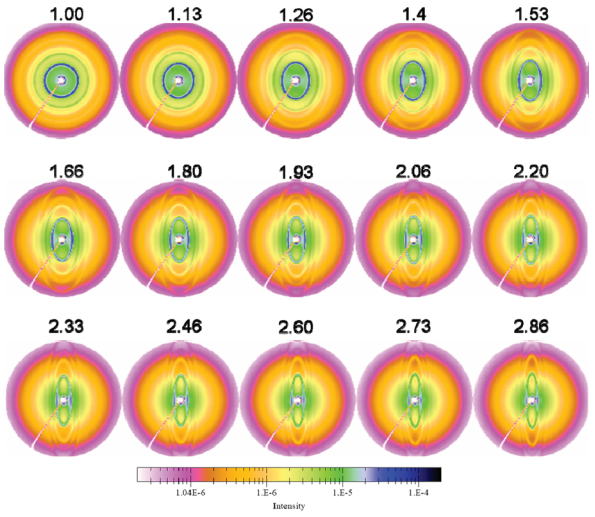

Figure 3. Selected SAXS patterns of uniaxially drawn latex films annealed for 20 min in solvent. The macroscopic draw ratio is indicated on each pattern. The tensile direction is horizontal.

the shift in the corresponding q positions from larger to smaller values can be attributed to the deformation of the latex film. Figure 2B shows a photograph of two crucibles for TGA experiments. It was clearly seen that the crucible for the annealed sample is much cleaner than that for the nonannealed sample, indicating that most of the salts and surfactants were dissolved and washed out of the latex film during the solvent annealing process. In light of this, the contrast of the films was decreased, resulting in a decrease in the scattering intensity with increasing annealing time. That means that the crystalline structure must be defined by the distribution of nonpolymeric material (e.g., salts and surfactants) between the particles

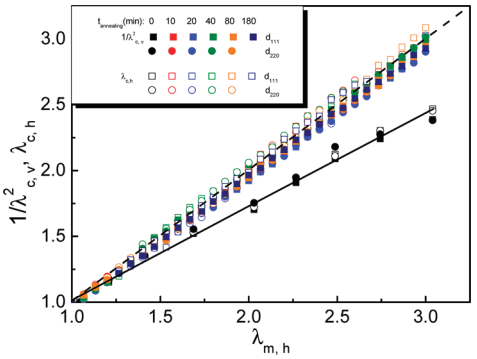

Figure 4. Crystallographic draw and compression ratios of the colloid crystallites along ($\lambda_{c,h}$) and perpendicular ($1/\lambda_{c,v}^2$) to the stretching direction as a function of the macroscopic draw ratio ($\lambda_{m,h}$) for samples before and after annealing in solvent for different durations. The dashed line indicates the behavior expected for affine deformation. The respective values are calculated from the shifts in the q positions of the Bragg peaks.

initially composing the film, in line with early observations made by Distler and Kanig.[31]

To elucidate the deformation behavior before and after solvent annealing, in situ SAXS measurements were conducted. Selected SAXS patterns taken at different draw ratios for latex films annealed for 20 min are given in Figure 3. It was found that the diffraction rings gradually became ellipses with increasing deformation, with the short axis in the stretching direction. The dimensions of the ellipses correspond to the inverse dimensions of the unit cell of the structure.[22] The microscopic deformation ratios, as indicated by the positions of the Bragg peaks, were derived from integrating the 2D SAXS patterns within a thin rectangular box along and perpendicular to the stretching direction. Shifts of the q positions parallel and perpendicular to the stretching direction after deformation for both cases can be directly read out from the data. To obtain the relationship between the microscopic deformation and the macroscopic deformation ratio, two diffraction peaks were followed during deformation except for the sample annealed for 180 min where only (111) diffraction was followed because the (220) diffraction in this sample became too diffuse. The corresponding draw and compression ratios of the crystalline lattices along and perpendicular to the stretching direction were plotted as a function of the macroscopic draw ratio in Figure 4.

It was found that the deformation was close to affine for samples before and after solvent annealing at small draw ratios (i.e., the macroscopic deformation was accomplished by the corresponding deformation of the colloidal crystalline structure). As reported previously,[25,26,28] this means that adhesive forces, originating from the coalescence of particles during the film-formation process between latex particles in the film, are strong enough to keep the entire film behaving as a homogeneous system with respect to the externally applied stress at small draw ratios. For nonannealed samples, a deviation from affine behavior was observed at large draw ratios, indicating that adhesive forces between latex particles in the film were not strong enough to prevent slippage in accordance with earlier work. Affine behavior over the whole range tested was obtained when the sample was solvent annealed. This deformational behavior has been explained as follows: solvent annealing promotes the interdiffusion of the polymeric chains across the boundaries of adjacent latex

dx.doi.org/10.1021/la2026939 |*Langmuir* 2011, 27, 12197–12200

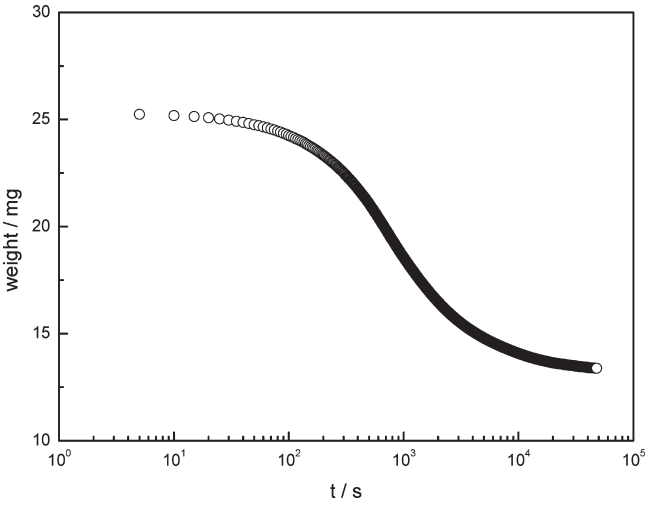

Figure 5. Weight change of a sample directly after 20 min of solvent annealing as measured by TGA.

particles, resulting in enhancing the cohesive bonding between latex particles in the crystalline lattice as well as at the crystalline grain boundaries. In turn, this effectively hinders the slippage of the rows of particles and also grain boundaries at large draw ratios, leading to affine deformation behavior. As is well known, the traditional approach to obtaining useful films from hard latex particles is to add a volatile organic solvent as a coalescing aid to the dispersion. The solvent acts as a plasticizer, lowering the modulus of the particles in the dispersion so that they deform upon drying and also promoting polymer diffusion in the film.[13] Unlike in the case of temperature annealing, as reported in our previous work, where a gradual increase in the degree of affinity of the microscopic deformation with respect to the macroscopic deformation is observed,[26,28] solvent annealing promotes a very significant effect. All films annealed in solvent exhibit affine deformation behavior regardless of the annealing time, indicating that via the swelling of latex particles solvent annealing induces the interdiffusion of polymeric chains in a more enhanced manner than thermal annealing. To elucidate this effect, the evaporation process of the 20 min solvent-annealed sample was measured, and the sample weight as a function of time is given in Figure 5. Clearly, complete solvent evaporation takes more than 10 h under ambient conditions, providing enough time for polymer chain interdiffusion between adjacent particles after annealing, which promotes stronger adhesive forces between particles.

CONCLUSIONS

The effect of solvent annealing on the deformation mechanism of styrene/*n*-butyl acrylate copolymer latex films subjected to uniaxial tensile deformation was investigated by in situ synchrotron SAXS. The deformation mechanism within the latex films transforms them from nonaffine deformation to affine deformation behavior after annealing in solvent. The transformation was attributed to the interdiffusion of polymeric chains between adjacent latex particles, resulting in an enhancement of the cohesive bonding between particles not only within crystalline domains but also at grain boundaries. It was found that solvent annealing introduces a more profound effect than thermal annealing because of the greatly enhanced interdiffusion of polymeric chains between adjacent latex particles.

AUTHOR INFORMATION

Corresponding Author
*E-mail: men@ciac.jl.cn.

ACKNOWLEDGMENT

This work was supported by the National Natural Science Foundation of China (51073159, 20874101, and 50921062) and the HASYLAB project (II-20080190).

REFERENCES

(1) Rieger, J.; Hadicke, E.; Ley, G.; Lindner, P. *Phys. Rev. Lett.* **1992**, *68*, 2782.
(2) Chevalier, Y.; Pichot, C.; Graillat, C.; Joanicot, M.; Wong, K.; Maquet, J.; Lindner, P.; Cabane, B. *Colloid Polym. Sci.* **1992**, *270*, 806.
(3) Roulstone, B. J.; Wilkinson, M. C.; Hearn, J.; Wilson, A. J. *Polym. Int.* **1991**, *24*, 87.
(4) Roulstone, B. J.; Wilkinson, M. C.; Hearn, J. *Polym. Int.* **1992**, *27*, 43.
(5) Wang, Y.; Juhue, D.; Winnik, M. A.; Leung, O. M.; Goh, M. C. *Langmuir* **1992**, *8*, 760.
(6) Keddie, J. L. *Mater. Sci. Eng., R* **1997**, *21*, 101.
(7) Winnik, M. A. *Curr. Opin. Colloid Interface Sci.* **1997**, *2*, 192.
(8) Steward, P. A.; Hearn, J.; Wilkinson, M. C. *Adv. Colloid Interface Sci.* **2000**, *86*, 195.
(9) Hahn, K.; Ley, G.; Schuller, H.; Oberthur, R. *Colloid Polym. Sci.* **1986**, *264*, 1092.
(10) Oh, J. K.; Yang, J.; Tomba, J. P.; Rademacher, J.; Farwaha, R.; Winnik, M. A. *Macromolecules* **2003**, *36*, 8836.
(11) Wang, Y. C.; Winnik, M. A. *Macromolecules* **1993**, *26*, 3147.
(12) Liu, Y. Q.; Haley, J. C.; Deng, K.; Lau, W.; Winnik, M. A. *Macromolecules* **2007**, *40*, 6422.
(13) Juhue, D.; Wang, Y. C.; Winnik, M. A.; Haley, F. *Makromol. Chem. Rapid Commun.* **1993**, *14*, 345.
(14) Kawaguchi, S.; Odrobina, E.; Winnik, M. A. *Macromol. Rapid Commun.* **1995**, *16*, 861.
(15) Ye, X. D.; Wu, J.; Oh, J. K.; Winnik, M. A.; Wu, C. *Macromolecules* **2003**, *36*, 8886.
(16) Kim, H. B.; Winnik, M. A. *Macromolecules* **1994**, *27*, 1007.
(17) Kim, H. B.; Winnik, M. A. *Macromolecules* **1995**, *28*, 2033.
(18) Juhue, D.; Lang, J. *Macromolecules* **1995**, *28*, 1306.
(19) Rharbi, Y.; Cabane, B.; Vacher, A.; Joanicot, M.; Boue, F. *Europhys. Lett.* **1999**, *46*, 472.
(20) Lepizzera, S.; Scheer, M.; Fond, C.; Pith, T.; Lambla, M.; Lang, J. *Macromolecules* **1997**, *30*, 7953.
(21) Oberdisse, J. *Macromolecules* **2002**, *35*, 9441.
(22) Rharbi, Y.; Boue, F.; Joanicot, M.; Cabane, B. *Macromolecules* **1996**, *29*, 4346.
(23) Men, Y. F.; Rieger, J.; Roth, S. V.; Gehrke, R.; Kong, X. M. *Langmuir* **2006**, *22*, 8285.
(24) Hu, S. S.; Men, Y. F.; Roth, S. V.; Gehrke, R.; Rieger, J. *Langmuir* **2008**, *24*, 1617.
(25) Hu, S. S.; Rieger, J.; Lai, Y. Q.; Roth, S. V.; Gehrke, R.; Men, Y. F. *Macromolecules* **2008**, *41*, 5073.
(26) Zhang, J. Q.; Hu, S. S.; Rieger, J.; Roth, S. V.; Gehrke, R.; Men, Y. F. *Macromolecules* **2008**, *41*, 4353.
(27) Zhang, J. Q.; Men, Y. F. *Chin. J. Polym. Sci.* **2009**, *27*, 49.
(28) Zhang, J. Q.; Hu, S. S.; Rieger, J.; Roth, S. V.; Gehrke, R.; Men, Y. F. *Macromolecules* **2009**, *42*, 4795.
(29) Hu, S. S.; Rieger, J.; Roth, S. V.; Gehrke, R.; Leyrer, R. J.; Men, Y. F. *Langmuir* **2009**, *25*, 4230.
(30) Hu, S. S.; Rieger, J.; Yi, Z. Y.; Zhang, J. Q.; Chen, X. L.; Roth, S. V.; Gehrke, R.; Men, Y. F. *Langmuir* **2010**, *26*, 13216.
(31) Distler, D.; Kanig, G. *Colloid Polym. Sci.* **1978**, *256*, 1052.